Supporting Information

Evolution of particle size distribution and solution composition in the PDF fits over time

Fig. 4 of the main text shows the evolution of the mean diameter, i.e. the crystalline domain sizes, of the ZnO ac and dmlt nanoparticles over time. In panel a of Fig. S1, the evolution of the crystalline domain size of cit is added as green squares. Along with the diameters, the fitted Gaussian size distributions are characterized by the width σ_{NP}, which are plotted in Fig. S1 b for the three different ligands ac, cit and dmlt. For ac and dmlt, in contrast to cit, data points were also collected after 900 and 1000 minutes of reaction time. These tend to indicate a steady state for dmlt, but a continued growth for ac. In case of ZnO dmlt, the nanoparticles can be stored in their dry powder form over several weeks without growth. [31] The slight trend of the *in-situ* data points indicating no growth at $t > 800$ min for dmlt is thus supported. In a separate study on the particle sizes in the dry powders (see Tab. S1†), ZnO ac was shown to undergo post-synthesis growth upon drying to a dry nanoparticle powder, confirming the tendency to grow also further in solution.

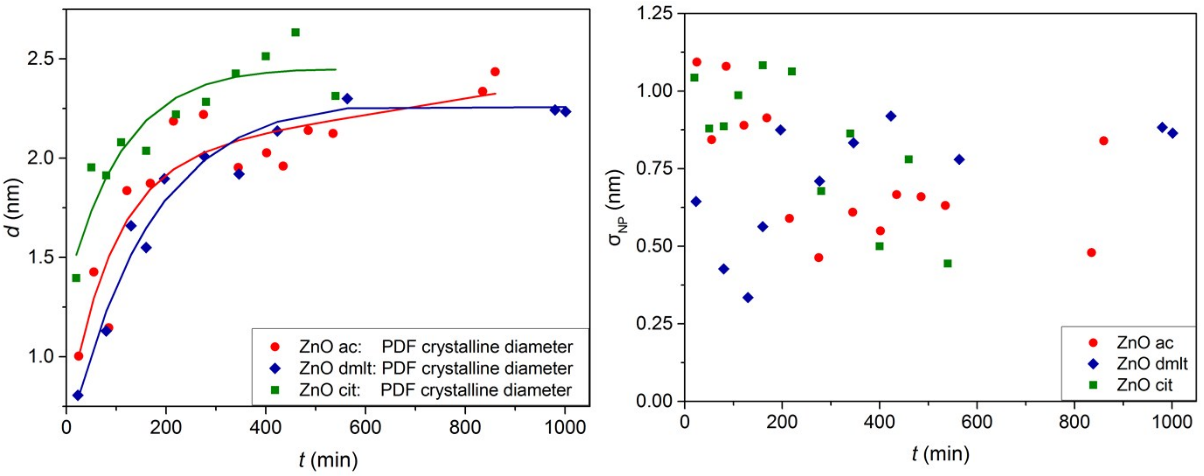

Fig. S1 Evolution of the crystalline domain size d and width σ_{NP} of the Gaussian size distribution of the ZnO nanoparticles capped with the three ligands ac (red dots), dmlt (blue rhombs) and cit (green squares). All nanoparticles seem to feature comparable polydispersity after 500 min, whereas thereafter the trend is not clear for ac. The large fluctuation of fitted values also emphasizes that the PDF technique is not ideal for determining the polydispersity. (Three data points were binned for each displayed data point and about every 20th dataset of each experiment was fitted.)

The polydisperse nanoparticles were fitted together with a precursor phase consisting of the tetrahedral Zn_4OAc_6 clusters. The fraction of Zn atoms contained within the precursor phase is shown in Fig. S2 for the three different ligands ac, cit and dmlt. ZnO cit immediately has the largest conversion rate to particles, i.e. the lowest remaining precursor fraction. Precursors in the ZnO ac reaction continue to react over time. ZnO dmlt shows the largest remaining precursor fraction. It should be kept in mind, that the tetrahedral precursor core Zn_4O is identical with a building block of wurtzitic ZnO nanoparticles. They both feature peaks in the PDF at 2 and 3.2 Å, which are the most dominant peaks in the d-PDFs overall. Moreover, a disordered nanoparticle, where neighbouring tetrahedrons are tilted against each other, also predominantly features those two peaks. Therefore, the fit cannot distinguish in between precursor phase and disordered nanoparticles or disordered regions within nanoparticles. It was shown that ZnO dmlt nanoparticles feature the largest degree of disorder as seen in the slow peak shifts and gradual crystallization in the PDFs over time (see Fig. 3 in the main text), which was found be to related to the strong binding of the dmlt ligand. The fit result for the number of precursor clusters for ZnO dmlt could hence be a true lower turnover rate of precursors to particles or just disordered nanoparticle domains, which are interpreted within the fit as an increased precursor fraction.

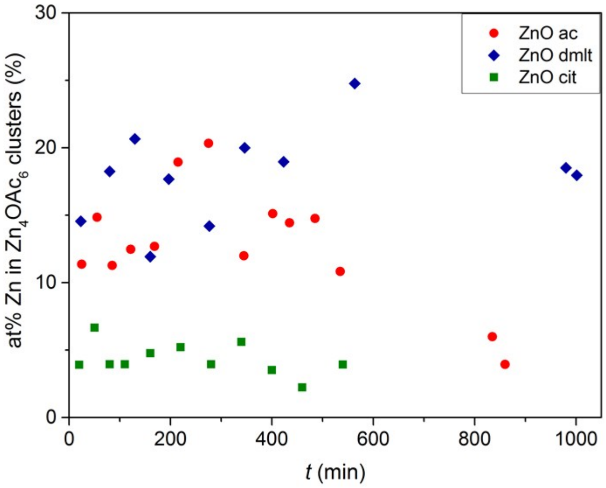

Fig. S2 Evolution of the solution composition, represented by the evolution of the atomic number fraction of Zn atoms contained within the tetrahedral precursor clusters Zn_4OAc_6, shown for three ligands: ac (red dots), cit (blue triangles) and dmlt (green rhombs). (Three data points were binned for each displayed data point and about every 20th dataset of each experiment was fitted.)

PDF peak shifts of 3.2, 5.6 and 8.6 Å peaks for acetate, citric acid and dmlt experiments

For all ligands, the 3.2 Å peak shows the least shift in its position (different y-axis scaling!), because the tetrahedral coordination is largely achieved directly after the base addition. The cit particles have the most wurtzitic structure after nucleation, since the peaks at 5.6 and 8.6 Å also hardly change their position. Ac-capped nanoparticles crystallize quite quickly, whereas ZnO dmlt needs extended periods of time till the disordered structure can adopt the crystalline phase. Even the appearance of the 5.6 and 8.6 Å peaks of dmlt seem to be delayed until ca. 20 and 60 minutes respectively.

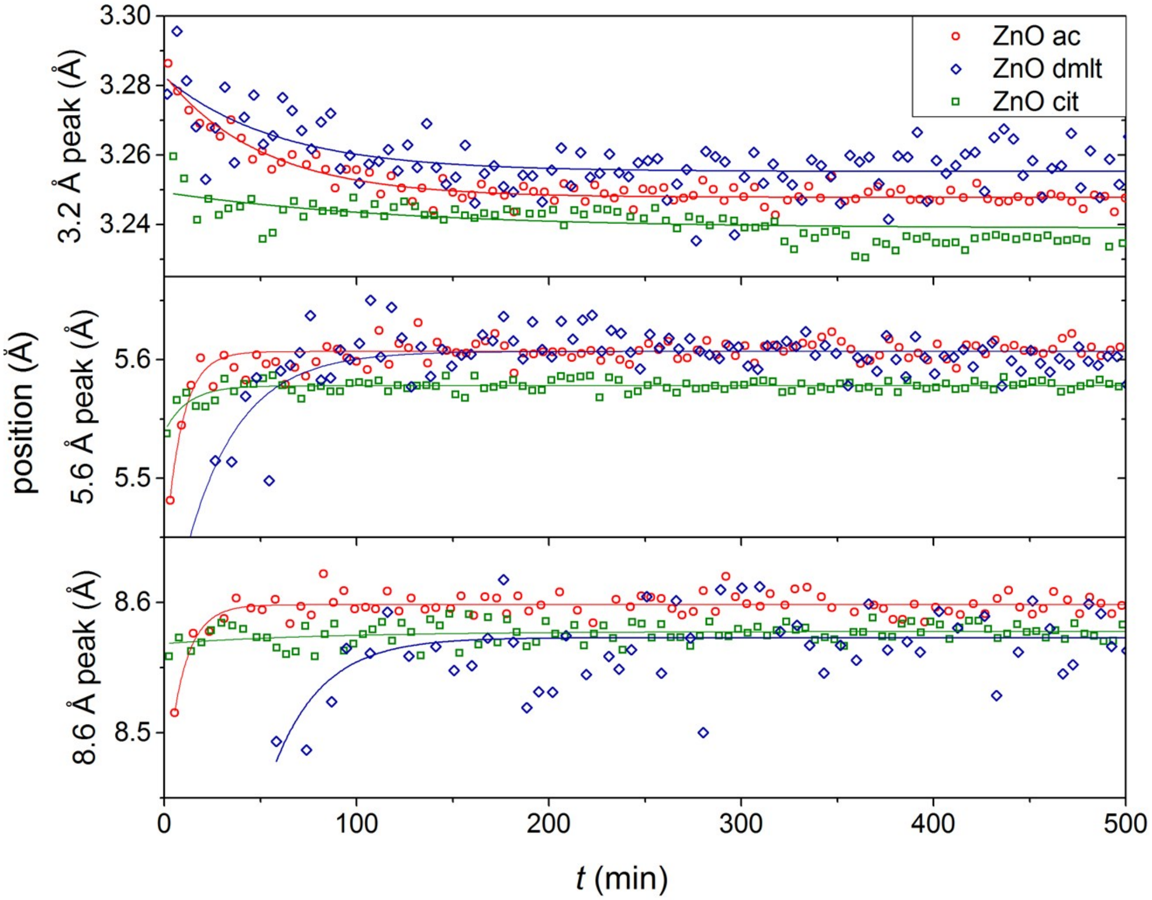

Fig. S3 Evolution of prominent PDF peak positions over time for ZnO nanoparticles with ligands ac (red circle), dmlt (blue rhomb) and cit (green square). The 3.2, 5.6 and 8.6 Å peaks are somewhat representative for the evolution of the short-range order of the particles, and furthermore possess the least peak overlap with others. All peaks shift asymptotically to a constant value, but with different rates. ZnO dmlt particles crystallize by far the slowest, indicated by the delayed appearance of the 5.6 and 8.6 Å peaks.

Contribution of nanoparticle, precursor and restructured solvent to d-PDF fits

Fig. S4 gives an example for the fits of the d-PDFs as they have been carried out for all data sets. The plot shows the experimental d-PDF of ZnO ac nanoparticles after 500 min reaction time (black) together with the final fit (red) and the difference curve (grey, in offset). The final fit consists of contribution from the polydisperse nanoparticles (green), the precursor (turquoise) as well as the restructured solvent (blue).

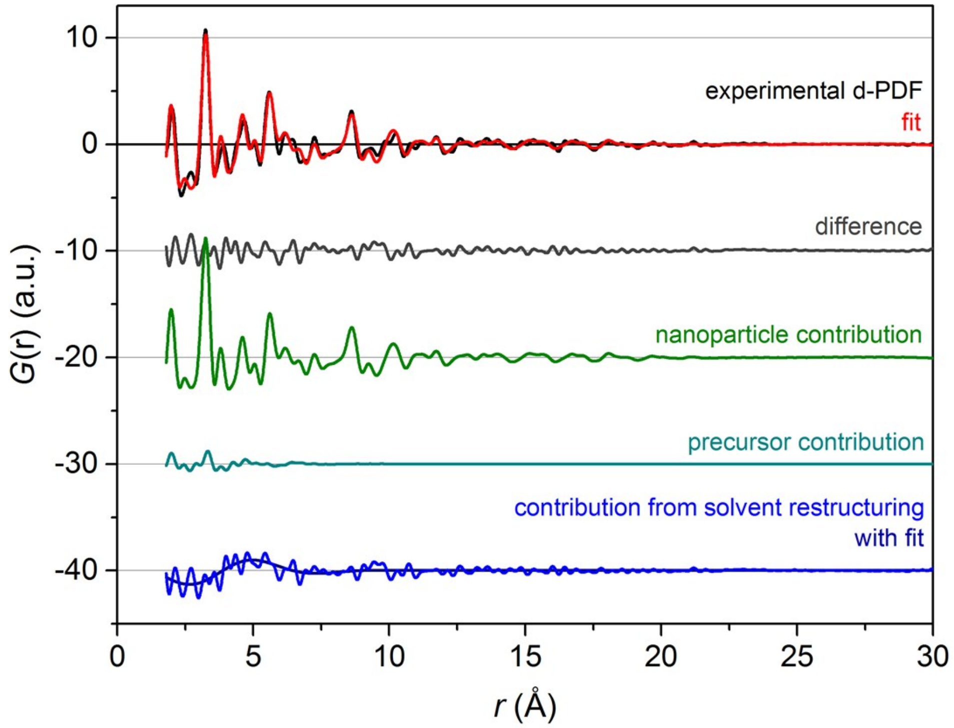

Fig. S4 Fit to the d-PDF of ZnO ac nanoparticles after 500 min reaction time in ethanol. Experimental d-PDF of ZnO ac nanoparticles (black) and their fit (red), showing the overall difference of the fit (grey, offset). The contribution of the nanoparticle (green) and the precursor (turquoise), as well as the contribution and fit of the restructured solvent (blue) are offset for the sake of clarity.

Assessment of differential PDFs confirmed from molecular simulation

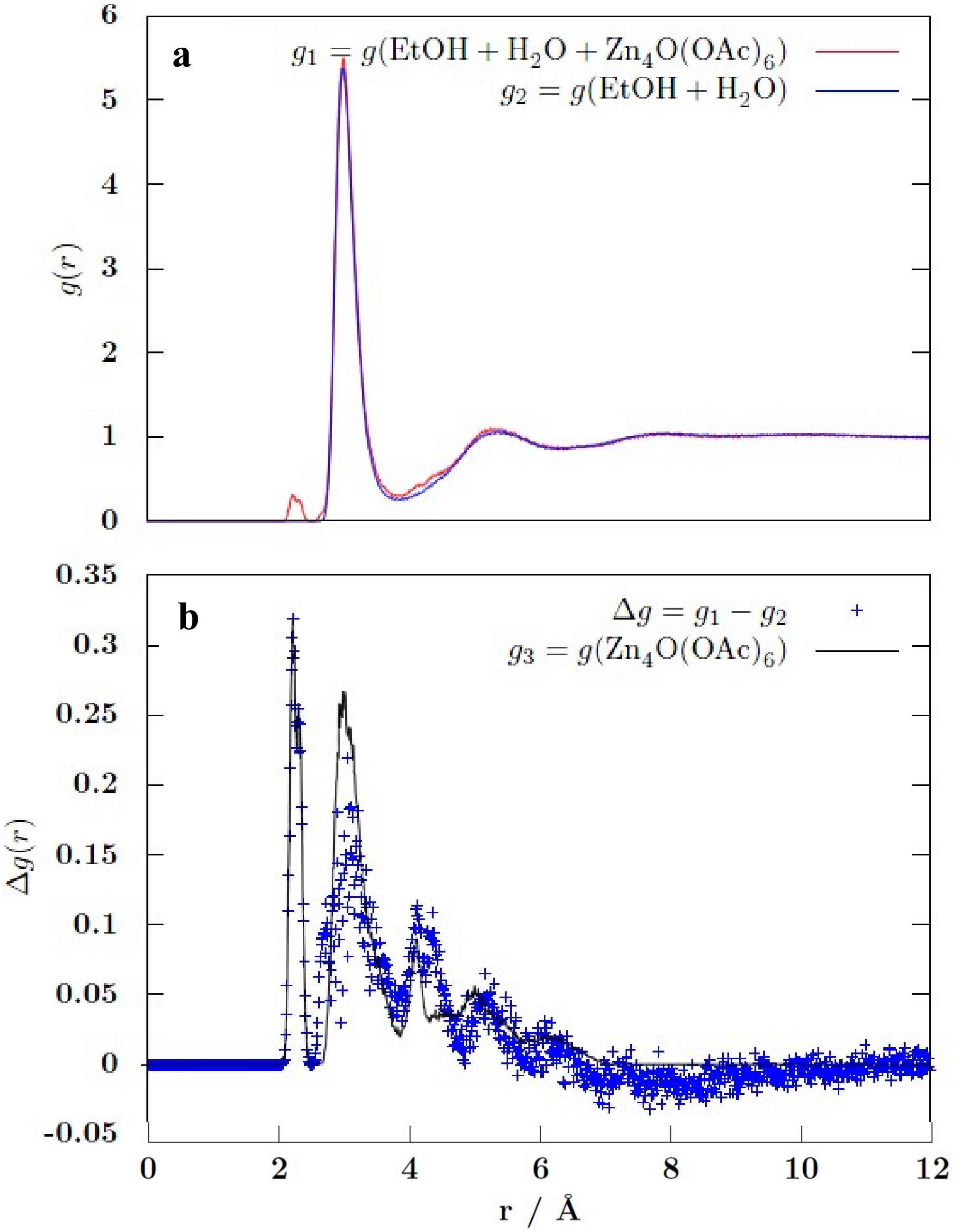

Fig. S5 (a) PDF of the Zn_4O-Acetate precursor in ethanolic solution as compared to the bulk solvent. (b) The differential PDF shows good agreement to the PDF from direct sampling of the ion-ion distances from the 10 ns molecular dynamics runs. This nicely confirms the background-correction used in experimental assessment of PDF data from XRD.

Contribution of different lognormal distributed particle size distributions to the SAXS fits

Depending on the organic ligand, up to three polydisperse lognormal distributions have been simultaneously fitted to the experimental data. An example of such a fit is shown for the ZnO ac system for *t* = 20 min after the TMAH addition.

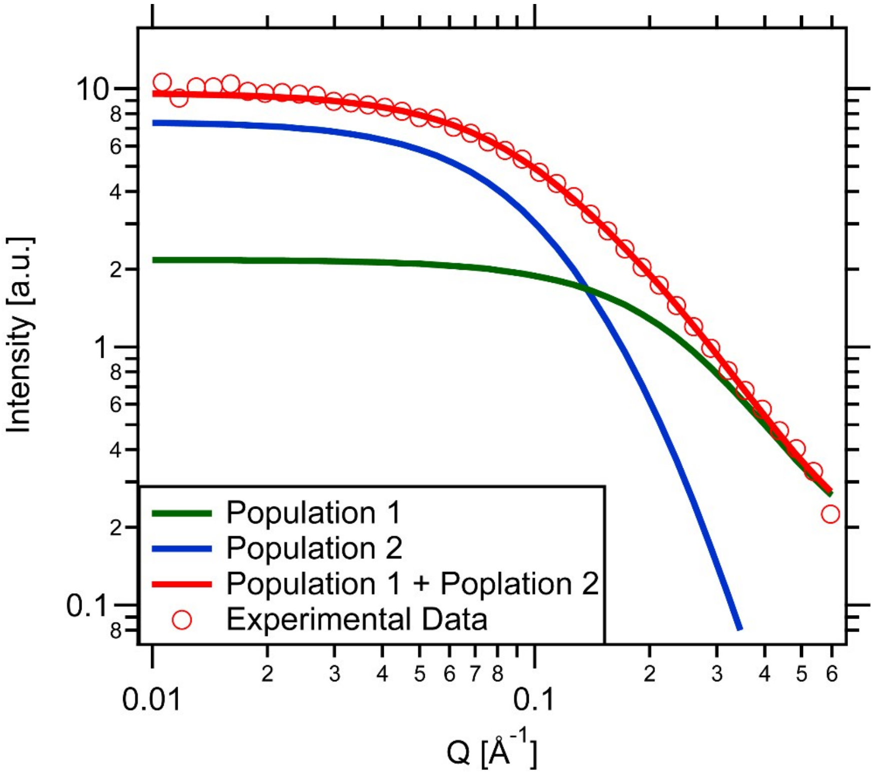

Fig. S6 Fit to the experimental SAXS curve of ZnO ac nanoparticles after 20 min reaction time in ethanol. Experimental data (red open circles) with overall fit (red solid line), showing the two fitted, individual populations of lognormal distributed particles as blue and green solid lines. The overall fit is the sum of the two individual populations.

Evolution of particle size distribution and solution composition in the SAXS fits over time

Fig. S7, S8 and S9 contain the SAXS fit results for the ligands ac, dmlt and pent. The panels show the particle diameters of the individual contributions (Population 1, 2 and occasionally 3) as well as a mean diameter. The mean diameter is calculated as the volume-weighted diameter of the individual populations. The corresponding total particle volume of the populations, which represents the solution composition, is displayed in panels b.

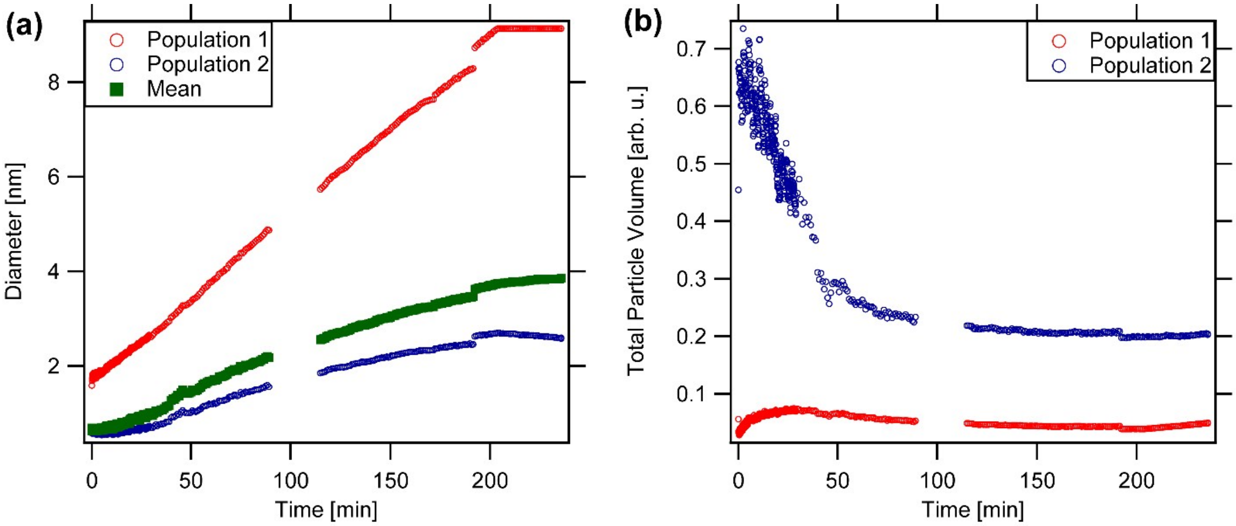

Fig. S7 Evolution of the mean and individual diameters (a) and total particle volumes (b) of the individual populations for ac. The missing data points between 90 and 115 min correspond to beam instabilities during the measurement, so that the acquired data could not be evaluated.

The gap in data points between 90 and 115 minutes for ZnO ac is due to a loss of the synchrotron beam during the experiment.

There are differences in the number of populations, which are needed to describe the SAXS curves. The ZnO ac system in Fig. S7 only demands two populations, whereas for dmlt in Fig. S8, a third population has to be introduced at t = 170 min. For dmlt, the increase in the diameter of this largest population is probably due to the formation of small agglomerates from individual particles and represents the size of agglomerates. The size difference of these agglomerates and the individual particle populations is less than one order of magnitude and the agglomerates form very gradually. More importantly, the volume fraction of this largest population is so small (see panel Fig. S8b) that it does not contribute significantly to the mean diameter. Thus, it was included in the calculation of the mean diameter. The small jump of the diameter and the volume of population 1 at t = 170 min is due to the introduction of the third population. The onset of slight agglomeration cannot be fixed to a specific point in time and it is most likely that very few agglomerates have existed before, which pretend a slightly larger diameter of population 1 before population 3 is introduced. As soon as these few agglomerates are modelled within the additional population, the particle size drops to a lower value representing the purely individual particles.

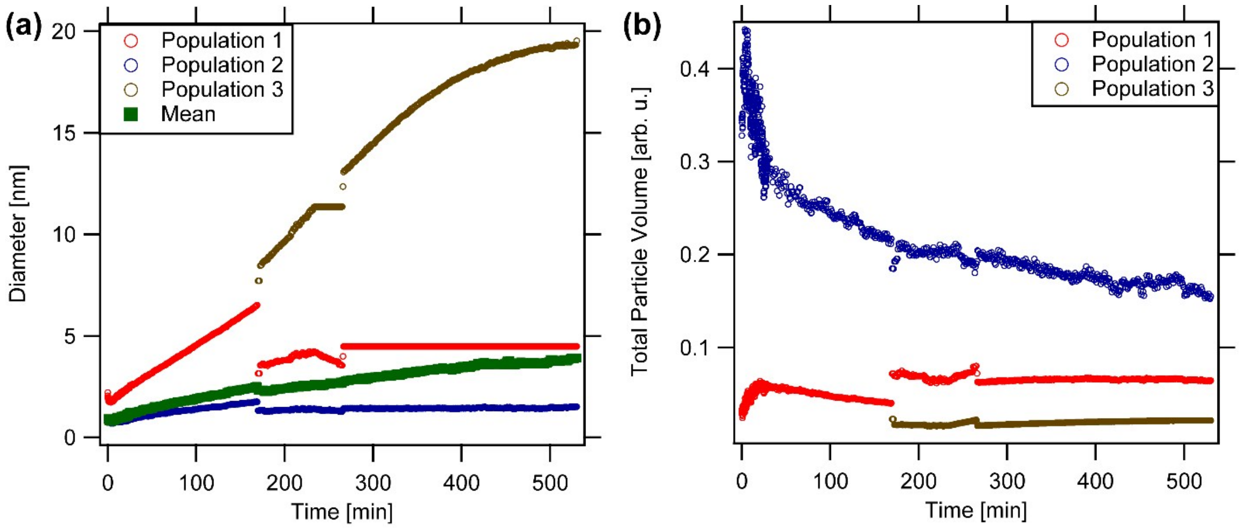

Fig. S8 Evolution of the mean and individual diameters (a) and total particle volumes (b) of the individual populations for dmlt.

As ZnO dmlt, the ZnO pent system also requires a third population to describe the data, see Fig. S9, for data points later than *t* = 70 min. Opposing to dmlt, this third population is an entire order of magnitude larger and can very clearly be associated to large aggregates (the y-axis is logarithmic). This is entirely in accordance with the macroscopic observation, that ZnO pent solutions turn cloudy and turbid spontaneously at some time after the TMAH addition. For pent, the largest population, i.e. the agglomerates, are not included into the mean diameter. Larger particles preferentially aggregate compared to smaller particles. Therefore, the strong decrease of the total particle volume of population 1 for *t* > 70 min corresponds to the amount of particles, which is incorporated into the aggregates.

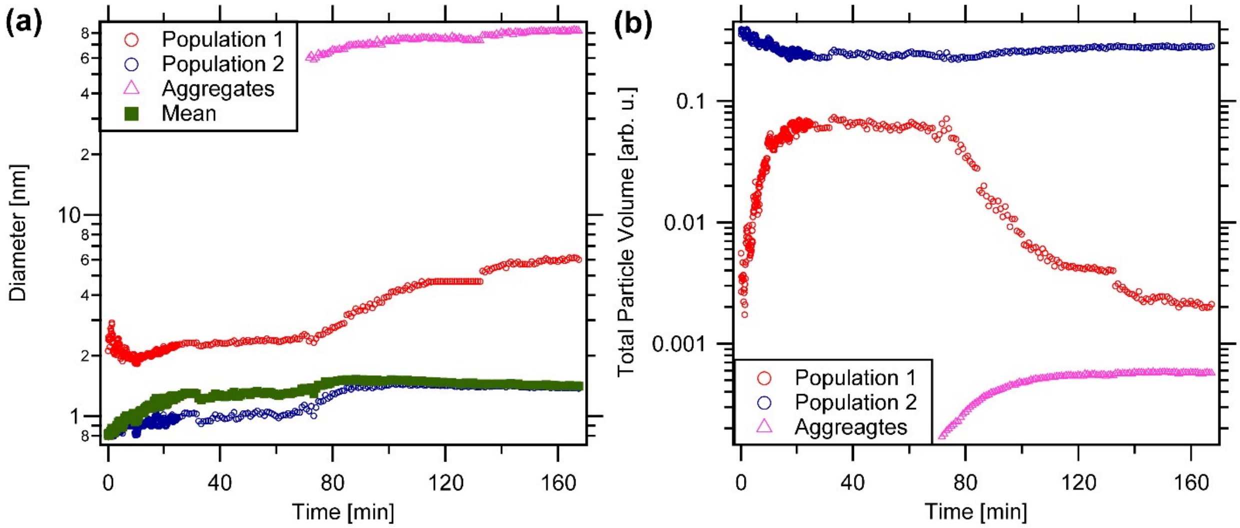

Fig. S9 Evolution of the mean and individual diameters (a) and total particle volumes (b) of the individual populations for pent on a logarithmic scale.

Particle size distributions in dry nanoparticle powders

The PDF refinements for the powders only included the modelling of nanoparticles with a Gaussian size distribution, because no precursor is contained within the powders.

Tab. S1 Sizes of nanoparticles in dry powders, given as the mean diameter d_0 of the Gaussian distribution with the width σ_{NP}

ligand	d_0 [nm]	σ_{NP} [nm]
ac	5.1	1.4
cit	3.1	0.9
dmlt	2.1	1.2
pent	3.2	0.2